

SEGMENTATION IN ECHOCARDIOGRAPHIC SEQUENCES USING SHAPE-BASED SNAKE MODEL

Chen SHENG

*Department of Communication
Mathematics and Science College
Shanghai Normal University
Shanghai, China
e-mail: chnshn@hotmail.com*

Yang XIN

*Institute of Image Processing and Pattern Recognition
Shanghai Jiaotong University
Shanghai, China
e-mail: yang.xing@sjtu.edu.cn*

Manuscript received 11 March 2005; revised 29 January 2007
Communicated by Steve J. Maybank

Abstract. A method for segmentation of cardiac structures especially for mitral valve in echocardiographic sequences is presented. The method is motivated by the observation that the structures of neighboring frames have consistent locations and shapes that aid in segmentation. To cooperate with the constraining information provided by the neighboring frames, we combine the template matching with the conventional snake model. It means that the model not only is driven by conventional internal and external forces, but also combines an additional constraint, the matching degree to measure the similarity between the neighboring prior shape and the derived contour. Furthermore, in order to automatically or semi-automatically segment the sequent images without manually drawing the initial contours in each image, generalized Hough transformation (GHT) is used to roughly estimate the initial contour by transforming the neighboring prior shape. Based on the experiments on forty sequences, the method is particularly useful in case of the large frame-to-frame displacement of structure such as mitral valve. As a result, the active contour can easily detect the desirable boundaries in ultrasound images and

has a high penetrability through the interference of various undesirables, such as the speckle, the tissue-related textures and the artifacts.

Keywords: Echocardiographic sequence, snake, generalized hough transformation, template matching

1 INTRODUCTION

Endocardial boundary detection in ultrasound images is a necessary step to obtain both qualitative measurements (i.e., the detection of pathological deformation) and quantitative measurements (i.e., area, volume etc.). Unfortunately, this is a difficult task due to the poor spatial and contrast resolutions, a high level of speckle noise etc. To overcome these problems, various algorithms are proposed to extract the boundaries of the region of interest (ROI) in echocardiographic images. These approaches can be mainly categorized based on Markov random field [5], artificial neural network [9], mathematical morphology [13] and deformable model [4], etc. In these schemes, the deformable model [7], which is also known as the snake model, is the most important and popular model for noisy and low contrast image segmentation. In this paper, the main reason for using the snake model is that it allows the incorporation of geometric constraints.

However, the conventional deformable models have some deficiencies for boundary detection in ultrasound images. First, the initial contour generally has to be placed quite close to the desirable boundary. Second, when the snake model is used to track the object in an image sequence by using the final contour from the previous frame as the initial contour in the current frame, the tracking works well only for small frame-to-frame displacement of anatomical structure [10]. Otherwise, the derived contour may be easily trapped in a local minimum formed by the noise. To remedy this problem, many techniques were proposed, for example, gradient vector flow (GVF) [14], dual snake [2] and discrete snake [11]. In this paper, it is noticed that the boundaries of any two adjacent images in a sequence are correlated to a certain degree. The result found in one image can be used as the shape template for the adjacent one. Thus, the only one rough shape template in a sequence needs to be given manually in the first step. For large frame-to-frame displacement of the structure, such as the mitral valve in the ROI, GHT is utilized to transform the shape template to an initial contour in the ROI. It has been proven that GHT is able to detect any arbitrary shape undergoing an affine transformation in an image [1].

Our method is based on template matching which incorporates the prior shape template which is the outline detected in the adjacent frame into the snake model. Optimizing the deformation energy between the shape template and the active contour, the shape of the active contour is constrained to be similar to the template in global while still allowing slight deformation locally.

2 METHODS

Let Ω be a bounded open subset of R^2 . Let $u_0 : \overline{\Omega} \rightarrow R$ be a given image, and $C(s) = (x(s), y(s))$ ($s \in [0, 1]$) be a parameterized contour with s being the parameter of length. The shape-based snake model is to minimize the following energy:

$$E(u_0, C_d, C_t) = \alpha E_{\text{int}}(C_d) + \beta E_{\text{ext}}(u_0, C_d) + \eta E_{\text{con}}(C_d, C_t) \quad (1)$$

where C_d is the active contour, C_t is the shape template.

$E_{\text{int}}(C_d)$ is the internal energy that controls the smoothness of the contour [7]:

$$E_{\text{int}}(C_d) = \int_0^1 |C'_d(s)|^2 ds + \int_0^1 |C''_d(s)|^2 ds. \quad (2)$$

$E_{\text{ext}}(u_0, C_d)$ is the external energy that attracts of the active contour evolving to the boundary of object. In this paper, it is calculated from the texture information instead of the local gradient in the ultrasound image. However, the blurred texture feature probably loses some object boundary information. Hence, the original image feature is also used to retain the boundary information. Let $T(x, y)$ denote the texture image after applying the texture analysis to the original image $u_0(x, y)$. The texture analysis of a point $P(x, y)$ is to calculate the average variance of the region, centered at point $P(x, y)$, with size of 3×3 pixels. The blurring Gaussian filter is applied to the texture image $T(x, y)$ to obtain the blurred texture image $T_G(x, y)$ (see Figure 1). Now the external energy E_{ext} is defined as:

$$E_{\text{ext}}(u_0, C_d) = -|\nabla u_0(C_d(s))| - |\nabla T_G(C_d(s))|. \quad (3)$$

Two terms on the right side of Equation (3) represent the gradient of the original image and the texture image, respectively.

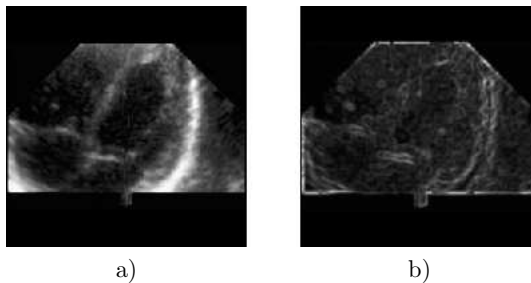


Fig. 1. a) original image; b) texture image blurred by Gaussian filter

$E_{\text{con}}(C_d, C_t)$ is the energy to measure the similarity between the active contour and the shape template. In this paper, our method has been inspired by the approach due to [6], where a scheme for matching two contours is proposed based on the

minimization of a quadratic fitting criterion, which consists of a curvature dependent bending energy term and a smoothness term.

The curvature is a key descriptor of the shape because it satisfies the following requirements:

1. The curvature is invariant under rotation and translation.
2. The curvature is a local and scale-dependent feature.

These allow to introduce a local bending energy measure of the form:

$$E_{curvature} = \int (k_{C_d}(s') - k_{C_t}(s))^2 ds. \quad (4)$$

where $k_{C_d}(s')$ is the curvature of the active contour C_d at s' as well as $k_{C_t}(s)$.

We also wish the displacement vector field to vary smoothly along the active contour:

$$E_{smooth} = \int \left\| \frac{\partial (C_d(s') - C_t(s))}{\partial s} \right\| ds. \quad (5)$$

So the criterion is composed of the curvature constraint and the smooth constraint:

$$E_{elastic} = E_{curvature} + \lambda E_{smooth} \quad (6)$$

where λ is a relative weighting factor (a high λ value means heavy smoothing). One of the successful choices for λ seems to be the heuristically defined adaptive weighting parameter as follows:

$$\lambda = \frac{1}{1 + k_{C_t}(s)}. \quad (7)$$

Duncan [6] finds a displacement field by direct minimization of a discrete form of Equation (6), the resulting displacement vectors in his approach may, however, map points not belonging to the two contours. This problem was solved by Cohen [3]. His mathematical model can be summarized as follows: Given two contours C_d and C_t parameterized by $s' \in [0, 1]$ and $s \in [0, 1]$, we have to determine a function $f : [0, 1] \rightarrow [0, 1]; s' \rightarrow s$ satisfying and

$$f(1) = 1 \quad (8)$$

and

$$f = \arg \min \{f1 \mapsto E_{elastic}(f1)\}. \quad (9)$$

Cohen [3] obtains the function f , which satisfies Equation (9) and conditions (8). It is obvious that it is complicated and difficult to solve. Our intention is to find a simplified equation, without losing the bending energy and smoothness requirements.

Equation (5) can be rewritten as:

$$E_{smooth} = \int \left\| \lim_{\Delta s \rightarrow 0} \left(\frac{\Delta C_d(s')}{\Delta s} - \frac{\Delta C_t(s)}{\Delta s} \right) \right\|^2 ds \quad (10)$$

According to the triangular inequality, we have:

$$\left\| \lim_{\Delta s \rightarrow 0} \left(\frac{\Delta C_d(s')}{\Delta s} - \frac{\Delta C_t(s)}{\Delta s} \right) \right\|^2 \geq \left(\lim_{\Delta s \rightarrow 0} \left(\left\| \frac{\Delta C_d(s')}{\Delta s} \right\| - \left\| \frac{\Delta C_t(s)}{\Delta s} \right\| \right) \right)^2. \quad (11)$$

In the limit, the arc length can be approximated as:

$$\lim_{\Delta s' \rightarrow 0} \Delta s' = \|\Delta C_d(s')\| \quad \lim_{\Delta s \rightarrow 0} \Delta s = \|\Delta C_t(s)\| \quad (12)$$

Substituting this relation in Equation (11), we get:

$$\int \left\| \frac{\partial (C_d(s') - C_t(s))}{\partial s} \right\|^2 ds \geq \int \left| \frac{\partial [f(s) - s]}{\partial s} \right|^2 ds \quad (13)$$

where $f(s) - s$ is the displacement due to the deformation.

Equation (12) establishes that the newly introduced smoothness term

$$E_{smooth} = \int \left| \frac{\partial [f(s) - s]}{\partial s} \right|^2 ds \quad (14)$$

is more simple and leads to a more simple equation:

$$E_{elastic} = \int (k_{C_d}(s') - k_{C_t}(s))^2 ds + \lambda \int \left| \frac{\partial [f(s) - s]}{\partial s} \right|^2 ds. \quad (15)$$

In this paper, the energy $E_{elastic}$ of template matching is treated as the global shape constraint E_{con} in Equation (1).

3 INITIALIZATION OF THE ACTIVE CONTOUR AND MINIMIZATION OF THE ENERGY

The shape template must be approximated as a vector containing a sequence of discrete points in order to solve by numerical method, $W = [w_1, w_2, \dots, w_n]$, where $w_i = (w_{ix}, w_{iy}) \in \{(x, y) : x, y = 1, 2, \dots, M\}$. The same method is used for the active contour, $V = [v_1, v_2, \dots, v_n]$.

Before processing the boundary detection by the snake, an initial contour must be drawn. The purpose of the initialization is to place the initial contour as close as possible to the boundary in ROI in order to obtain a fast convergence in the

boundary detection. In this paper, the GHT is applied to solve this problem. Let us define a geometric transformation of the shape template by [12]:

$$V = AW + t = \begin{bmatrix} a_A & b_A \\ c_A & d_A \end{bmatrix} \cdots \begin{bmatrix} W_x \\ W_y \end{bmatrix} + \begin{bmatrix} t_x \\ t_y \end{bmatrix} \quad (a_A d_A - b_A c_A \neq 0) \quad (16)$$

where A and t correspond to a linear transformation and to a translation vector, respectively. The potential location of the position parameters t for the potential parameters A of the linear transformation can be expressed as $t(W, V, A) = V - AW$. This method traces an initial contour in the parameter space, and after gathering all evidence for all ROI pixels, the maximum of the accumulator array defines the best values A^* and t^* which correspond to the transformation that maps the shape template to the echocardiographic image. The GHT can deliver a reliable estimation of the ROI position or a coarse initial contour.

During minimization of Equation (1), the ideal approach is to search every point in the region of interest to get the vector $\bar{V} = \{\bar{v}_1, \bar{v}_2, \dots, \bar{v}_n\}$. However, the complexity of this algorithm in $O(nm^3)$ increases rather rapidly with m (m is the number of points within the search region, n is the number of points to represent the contour). During searching optimization contour process, each point is evolving in the search region. It is not only influenced by its own, but also by the other $n - 1$ points; so the complexity is m^n , and, for all the n points, the complexity is nm^n . In order to reduce the complexity, we assume that the evolving result of one point be influenced only by the two adjacent and its own points; so the complexity is m^3 and the whole complexity for contour is nm^3 .

Here a search strategy is adopted to encompass large search regions without drastically increasing m . The basic idea is to concentrate the initial search in regions that will more likely yield the solution, instead of spreading them out evenly [8].

In the initial stage, we desire to rapidly inflate or deflate parts of V to locate the neighbourhoods of the global minimum. This can be achieved by searching in the normal directions of v_i .

The region of searching is: $\Theta = \bigcup_{i=1}^n \Theta_i$, where Θ_i contains all the points on the normal vector h_i . $\Theta_i = \{\bar{v}_i = v_i + kh_i; k = 0, \pm 1, \dots, \pm \frac{m-1}{2}\}$, m is odd.

In this paper, the stratified line search algorithm was used: $\Theta_i = \bigcup_{j=1}^{m/l} \Theta_{ij}$, $\Theta_{ij} = \{\bar{v}_i = v_i + (l_j + k)h_i; k = 0, \pm 1, \dots, \pm \frac{l-1}{2}\}$ l is odd, and the complexity is $O(nm^3/l^2)$.

The stratified line search is performed in the initial stage of minimization to quickly locate the regions, which contain the global minimum. This can then be followed by basic line search and completed by searching in 3×3 regions.

3.1 Experiments and Results

In this section, several examples are presented to illustrate the efficiency of the shape-based snake model for boundary detection in echocardiographic sequences. Forty sequent ultrasound images with size 180×180 pixels were obtained from the Philip 5500 system, each covering one complete cardiac cycle and containing $F = 16$ frames. The algorithm has been implemented using an Intel Pentium IV 2.4 GHZ with 1 GB RAM, under the Visual C++ 6.0 environment.

To assess the performance of our segmentation method, we compared automatically detected cardio structure boundaries with the manual outlines. In this paper, four sets of manual outlines are given for each of the sequences.

Two sets of parameters are employed: the mean, the standard deviation (SD), and the maximum of the minimal distances from the derived boundary points to the manual outline. They are used to measure the difference between the derived contour and the outline in one frame of a sequence. Let C_d and C_m denote the derived contour and the manual outline, respectively.

1. For each $p_i \in C_d$, find $p_i^* \in C_m$ so that $p_i^* = \arg \min_{\forall p_j^* \in C_m} \|p_i - p_j^*\|$, where $\|p_i - p_j^*\|$ means the Euclidean distance between the two pixels.
2. For all (p_i, p_i^*) , compute the Euclidean distance d .
3. Compute the mean, the SD and the maximum of $\{d \mid \forall p_i \in C_d\}$.

We need another set of parameters to evaluate the segmentation results for the whole sequence, so the mean and the SD of the mean absolute distance (MAD) are defined as follows:

1. The MAD between two contours A and B is defined as:

$$D(A, B) = \frac{1}{2} \left\{ \frac{1}{n} \sum_{i=1}^n d(a_i, B) + \frac{1}{m} \sum_{i=1}^m d(b_i, A) \right\}.$$

2. Compute the mean, the SD of $\{D \mid \forall D \in S\}$, where S is all the MADs need to be calculated for a sequence.

3.2 Process of Segmentation

For a 2-D echocardiographic sequence, we first obtained the initial contour of the image k using our algorithm. The final contour of the image k is obtained after the deformation process, which is then transformed by GHT in order to be treated as the initial contour of the next image $k + 1$. That is, the final contour of the k^{th} image is taken to be the initial contour of the $(k + 1)^{\text{th}}$ image, and so on. By this method, all initial contours can be obtained from the final contours of the previous images.

Figure 2 shows the segmentation process for a mitral valve sequence. The initial contour of the $(k + 1)^{\text{th}}$ image obtained directly from the final contour of the k^{th} image is shown in Figure 2 c). Figure 2 b) presents the initial contour, which has been transformed by GHT. In Figure 2 d) we can see that the segmentation result rather coincides with the contour manually defined by an independent doctor in Figure 2 e) when using GHT to locate the initial contour. On the other hand, we can see that the shape-based snake model treats well when there is a gap in the tip of the leaflet under the shape constraint. It may be reasonable to say that the segmentation result closely follows the desired boundary. Nevertheless, the algorithm fails when using the initial contour in Figure 2 c) because of trapping in a local minimum, although the same energy weighting factors ($\alpha = 1.0$, $\beta = 1.0$, $\eta = 0.5$) are given.

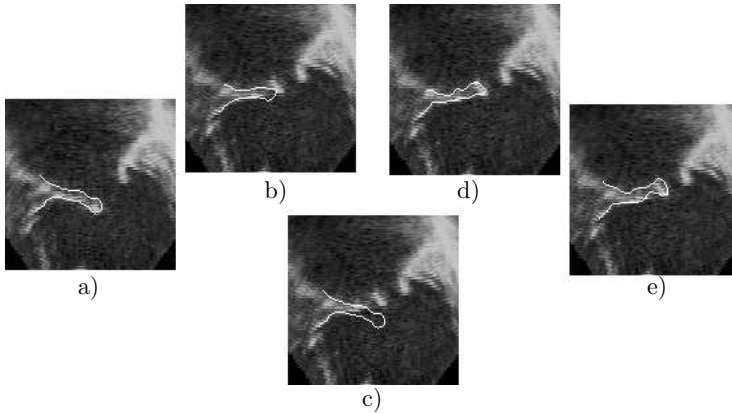


Fig. 2. Example of segmentation for mitral valve; a) the k^{th} image with final contour; b) the $(k + 1)^{\text{th}}$ image with initial contour from the k^{th} image using GHT; c) the $(k + 1)^{\text{th}}$ image with initial contour direct from the k^{th} image; d) the $(k + 1)^{\text{th}}$ image with segmentation result using initial contour in b); e) manual outline for the $(k + 1)^{\text{th}}$ image

GHT is not needed in all situations such as the small frame-to-frame displacement of the structure. Figure 3 e) shows the segmentation result for the left ventricle with the initial contour direct from the previous image is identical to that using GHT to locate the initial contour (Figure 3 d)). The evaluated parameters of the segmentation results are shown in Table 1. Both the mean and the SD of the minimal distances are near to each other.

Based on the experiments on forty sequences, it was indicated that when the displacement of the structure in the adjacent two images is larger than half the size of itself, the use of GHT to estimate the initial contour could achieve more satisfactory result.

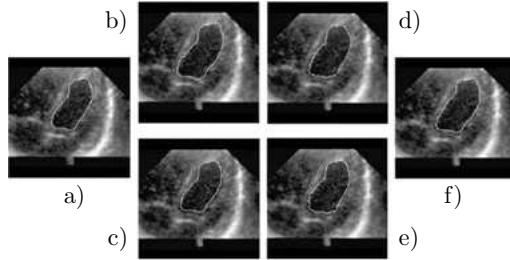


Fig. 3. Example of segmentation for left ventricle; a) the k^{th} image with final contour; b) the $(k+1)^{\text{th}}$ image with initial contour from the k^{th} image using GHT; c) the $(k+1)^{\text{th}}$ image with initial contour direct from the k^{th} image; d) the $(k+1)^{\text{th}}$ image with segmentation result using initial contour in b); e) the $(k+1)^{\text{th}}$ image with segmentation result using initial contour in c); f) manual outline for the $(k+1)^{\text{th}}$ image

Minimal distances	Mean [?]	SD [?]	Max [?]
Using GHT	1.5	1.06	5.2
Without using GHT	1.4	1.15	5.1

Table 1. The mean, the SD and the maximum of the minimal distances for Figure 3

3.3 Segmentation of Endocardial Boundaries in Sequences

In twenty sequences, the algorithm was used to segment the endocardial boundaries. Some frames from the first sequence are shown in Figure 4.

Four sequences selected, Table 2 shows the mean and the SD of the MADs for the whole sequence between the algorithm-generated contours and the four sets of manual outlines (the number of MADs needs to be calculated is $F \times m$, where F is the number of frames in the sequence and m is the number of manual outlines for each frame) and between different manual outlines (the number of MADs needs to be calculated is $F \times C_m^2$). These experiments show that the segmentation results compare well to the manual outlines for the endocardial boundaries.

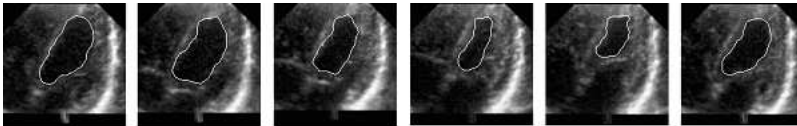


Fig. 4. Characteristic frames showing the segmentation results of the left ventricle

	Seq1	Seq2	Seq3	Seq4
Mean of MADs between snake and outlines [?]	1.22	1.75	1.61	1.18
SD of MADs between snake and outlines [?]	0.26	0.35	0.45	0.31
Mean of MADs between different manual outlines [?]	1.32	1.65	1.41	1.24
SD of MADs between different manual outlines [?]	0.22	0.34	0.30	0.28

Table 2. Results of the comparison between the algorithm-generated contours and the manual outlines

3.4 Segmentation of Mitral Valve Sequences

The algorithm performance was evaluated on twenty sequences of long axis view images of the mitral valve. Characteristic frames from the first sequence are shown in Figure 5. As one could expect, the differences of ROI between any two adjacent frames are larger, but the algorithm performance is still comparable to the manual segmentations. Table 3 shows the evaluated results for two selected mitral valve sequences. In this table we can see that the mean and the SD are larger than those in Table 2. This may be ascribed to at least two factors. The first one is that the manual outlines may vary with experts. The second factor is that the contours in the mitral valve images are open. The starting and the ending points defined by the experts may vary largely. As a result, the MAD between the open contours may be larger than that between closed contours.

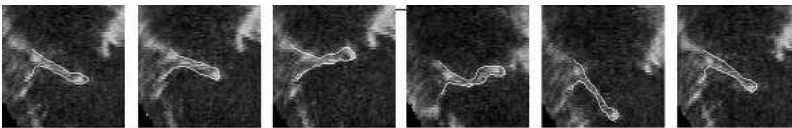


Fig. 5. Characteristic frames showing the segmentation results of the mitral valve

	Seq1	Seq2
Mean of MADs between snake and outlines [?]	2.14	2.02
SD of MADs between snake and outlines [?]	0.71	0.56
Mean of MADs between different manual outlines [?]	1.81	1.63
SD of MADs between different manual outlines [?]	0.69	0.52

Table 3. Results of the comparison between the algorithm-generated contours and the manual outlines for sequences containing images of the mitral valve

3.5 Determination of Weighting Factors

In our experiments, the weighting factors α, β, η are set in Table 4. The motion of the mitral valve is very irregular, frame-to-frame displacements are several times

larger than the leaflet thickness. At those phases, the leaflet rotates, translates and deforms at the same time. As a result, the difference of shape between two adjacent images may be large. So, for the mitral valve sequences, the constraint energy weighting factor is set lower than that for the others.

	α	β	η
Endocardial sequences	1.0	1.0	2.0
Mitral valve sequences	1.0	1.0	0.5

Table 4. Values of parameters used in the algorithm

GHT algorithms are known to be computationally expensive [12] (about 6 min for a sequence in our experiments) and they are not needed in all situations. So, in our method, the GHT was separated from the snake deformation process. A user can intervene when or where to use GHT. However, these algorithms do not need user's supervision during the segmentation process. The user's interaction was needed in just one frame for a sequence.

4 CONCLUSIONS

In this paper, an innovative model has been proposed for echocardiographic image segmentation, namely, the shape-based snake model. The proposed shape-based model aims at incorporating the template matching and the GHT with the snake model. The model can resist the speckle noise, tissue-related textures and artefacts, and guide the active contour deform to the desirable boundary. The principal idea of this model is to use GHT to estimate the initial contour, and then using the elastic deformation energy between the shape template and the active contour to guide the contour deform from the local minimum. Our method does not need to draw a precise shape template, but rather a rough contour regardless of its position, scaling and rotation only once in a sequence.

REFERENCES

- [1] BALLARD, D. H.: Generalizing the Hough Transform to Detect Arbitrary Shapes. *Pattern Recognition*, Vol. 13, 1981, pp. 111–122.
- [2] CHEN, C. M.—LU, H. H. S.: A Dual-Snake Model of High Penetrability for Ultrasound Image Boundary Extraction. *Ultrasound Med Biol*, Vol. 27, 2001, No. 12, pp. 1651–1665.
- [3] COHEN, I.—AYACHE, N.—SULGER, P.: Tracking Points on Deformable Curves. *Proc. Second Euro. Conf. Computer Vision 1992*, Santa Margherita Ligure, Italy, May 1992.
- [4] COOTES, T. F.—HILL, A.—TAYLOR, C. J.—HASLAM, J.: Use of Active Shape Models for Locating Structures in Medical Images. *Image Vis. Computing*, Vol. 12, 1994, No. 6, pp. 355–365.

- [5] DIAS, J. M. B.—LEITAO, J. M. N.: Wall Position and Thickness Estimation from Sequence of Echocardiographic Images. *IEEE Trans. on Medical Imaging*, Vol. 15, 1996, pp. 25–38.
- [6] DUNCAN, J. S.—OWEN, R.: Shape-Based Tracking of Left Ventricular Wall Motion. *Computers in Cardiology*, IEEE Computer Society, Chicago, Illinois. 1990 September, pp. 23–26.
- [7] KASS, M.—WITKIN, A.—TERZOPOULOS, D.: Snakes: Active Contour Models. *International Journal of Computer Vision*, Vol. 1, 1987, pp. 321–331.
- [8] KOK, F. L.—ROLAND, T. C.: Deformable Contours: Modeling and Extraction. *IEEE Trans PAMI*, Vol. 17, 1995, No. 11, pp. 1084–1090.
- [9] KOTROPOLULOS, C.: Nonlinear Ultrasonic Image Processing Based on Signal-Adaptive Filters and Self-Organizing Neural Networks. *IEEE Trans. Image Processing*, Vol. 3, 1994, pp. 65–77.
- [10] LEYMARIE, F.—LEVINE, M. D.: Tracking Deformable Objects in the Plane Using an Active Contour Model. *IEEE Trans. Pattern Analysis and Machine Intelligence*, Vol. 15, 1993, pp. 617–634.
- [11] LOBREGT, S.—VIERGEVER, M. A.: A Discrete Active Contour Model. *IEEE Trans. Medical Imaging*, Vol. 14, 1995, pp. 12–24.
- [12] SER, P. K.—SIU, W. C.: A New Generalized Hough Transform for the Detection of Irregular Objects. *Journal of Visual Communication and Image Representation*, Vol. 6, 1995, No. 3, pp. 256–264.
- [13] THOMAS, J. G.—PETERS, R. A.—JEANTY, P.: Automatic Segmentation of Ultrasound Images Using Morphological Operators. *IEEE Trans. Medical Imaging*, Vol. 10, 1991, pp. 180–186.
- [14] XU, C.—PRINCE, J. L.: Snakes, Shapes, and Gradient Vector Flow. *IEEE Trans. Image Processing*, Vol. 7, 1998, pp. 359–369.



Chen SHENG is an instructor in Mathematics and Science College of Shanghai Normal University and he also was a senior researcher and project leader in Kodak R & D center. He received his Ph.D. degree in computer science from Shanghai Jiaotong University and his M. Sc. degree in computer science from Xidian University. His research interest includes medical image processing, medical image retrieval, pattern recognition and computer aided diagnosis (detection), etc. He is author and co-author of several scientific papers.



Yang Xin is the vice director of the Image Processing and Pattern Recognition Institute of Shanghai Jiaotong University, and he also is a professor in the Department of Automation. He received his Ph. D. degree in computer science from VUB (The Free University of Brussels) and his M. Sc. degree in computer science from Northwestern Polytechnical University. His research interest includes medical image processing, 3D medical data processing, etc. He is supervisor for Ph. D. master studies.